Boichot R., Luo L., and Fan Y. Tree-network structure generation for heat conduction by cellular automaton. Energy Conversion and Management, 50(2):376–386, 2009.

# Tree-Network Structure Generation for Heat Conduction by Cellular Automaton

**Raphaël BOICHOT, Lingai LUO*, Yilin FAN**

Laboratoire Optimisation de la Conception et Ingénierie de l'Environnement (LOCIE),

Université de Savoie, Campus Scientifique, Savoie Technolac, 73376,

Le Bourget-Du-Lac cedex, France

## Abstract

This study proposes a cellular automaton approach to deal with the typical "area-to-point" problem of how to effectively cool a heat generating surface by arranging the configuration of high conductivity material links which discharges the generated heat to a heat sink. To demonstrate the principle and the procedure of the cellular automaton approach, a simple case of square surface with single heat sink is treated: the approach starts with an initial shape of a certain quantity of high conductivity material. By shaping the initial conductive drain trough the equipartition of thermal gradients, the high conductivity material evolves step-by-step and forms at convergence a final configuration, which turns out to be a multi-scale tree-like network. The effects of the conductivity ratio $\hat{k}$, the fraction of high conductivity material $\phi_0$ as well as the influence of the initial shape are discussed. The cellular automaton approach, which allows increasing the effective overall thermal conductance of an area, is fast, easy to apply and nearly constraint-free. Finally, the present limitations of the cellular automaton are also exposed.

*Corresponding author. Lingai LUO*
*Address : LOCIE –Université de Savoie, Campus Scientifique, Savoie Technolac, 73376, Le Bourget-Du-Lac cedex, France Tel.: 33479758193; fax: 33479758144.*
*E-mail address: Lingai.LUO@univ-savoie.fr*
*Author's new address: Raphaël BOICHOT*
*Laboratoire de Science et Ingénierie des Matériaux et Procédés (SIMAP). Grenoble INP, Domaine Universitaire, 1130 Rue de la Piscine BP75, 38042 Saint Martin d'Hères, France*
*E-mail address: raphael.boichot@ltpcm.inpg.fr*

Boichot R., Luo L., and Fan Y. Tree-network structure generation for heat conduction by cellular automaton. Energy Conversion and Management, 50(2):376–386, 2009.

**Keywords**: Cellular automaton, Heat conduction, Tree network, “aero-to-point” problem, Constructal.

## 1. Introduction

In electronic engineering or micro-electronic devices, the issue of how to cool the continuous heat generating volume (or surface) has raised more and more attention. One possible solution is based on adding certain quantity of high conductivity material in the heating surface to discharge the generated heat to a heat sink by heat conduction. The cooling effectiveness depends not only on the quantity (fraction) and quality (conductivity) of high conductivity material but also on the geometrical arrangement of high conductivity link. To solve this problem requires the introduction of Multi-Objective Optimization (MOO) approaches. This conductive cooling problem, which is in the category of a more general “area to point” flow problem, was analyzed by Bejan [1] by minimizing the thermal resistance of the heat generating area to maintain a limited maximum temperature on the area. It is reported that an optimal configuration for heat conduction from an area to a point-like sink minimizes resistance to heat conduction through the emergence of tree network structures-this is almost one of the earliest and basic work of constructal theory and its extensions [2, 3]. Bejan [1, 3] gave the optimal allocation of a conductive path or link to cool a 2D square heater starting from rectangular elemental areas. His study was recently revised and modified by Wu et al. [4] to obtain exact solutions. Rocha et al. [5] extended this concept to a disc-shape area to be cooled by heat conduction. Godhossi [6] and Godhossi and Egrican [7] attempted to use triangular elemental areas instead of the rectangular ones for the following assemble procedure according to constructal theory. Other authors like Zhou et al. [8] – with variable thickness conductors – and Lorenzini and Rocha [9] – with

variable angle elbows – began to add degrees of freedom during the elaboration of branched structures.

Similar principle was also applied to deal with the river drainage basins problem with the idea of infinite freedom to morph initiated by Ledezma et al. [10]. An important work on this subject is provided by Errera and Bejan [11] (cited from [2]). The method presented in their paper consists in pulling blocks out of a wet terrain if they are situated at a place where pressure gradient is superior to a given critical value. By increasing the flow rate of water wetting the terrain, a drainage tree-network progressively emerges. Three interesting features of this work are as follows. Firstly, freedom to morph is here nearly infinite by the definition of tiny elemental areas or cells. Secondly, the criterion of gradient was employed for morphogenesis. Thirdly, contrary to the classical constructal's principle that oblige to start from the area to go to the point, the approach of Errera and Bejan constructs the tree-network structure from the point (sink) to every elemental area of the whole domain. This approach with above three features simulates will the realistic dendritic patterns of river basin "area to point" system, with a finite complexity. However, in spite of the great application potential, this concept has been largely under-exploited in our opinion.

Following the early success of Errera and Bejan [11], our work aims to attack the conductive surface cooling problem by using a cellular automaton algorithm simulating the morphing by gradients. That is, for an initial shape of a certain quantity of high conductivity material, the cellular automaton proposed here changes the structure of the highly conductive link by automatically displacing elements of high conductivity material from regions of low thermal gradients to regions of high thermal gradients,

along the frontier between the two materials. And step-by-step, the thermal gradients at the frontier between the two materials are equalized and the final configuration emerges at the convergence. Constructal dichotomic tree with perpendicular branches and unspecified drains are employed as initial shapes. The decrease in maximum temperature of the area, the effects of the conductivity ratio $\hat{k}$, the fraction of high conductivity material $\phi_0$ as well as the influence of the initial shape will be discussed in detail in the following sections.

Actually, the use of cellular automata in science is not new (see Wolfram [12] for cellular automata examples) but their application, in the field of heat transfer optimization, is in our belief original.

## 2. Cellular automaton

To demonstrate the principle and the procedure of the cellular automaton approach, a simple case of square surface with single point-like heat sink is treated in this study. The square domain to cool is divided into small square elemental cells. Then the heat equation with volume heat production is solved at every elemental cell to obtain the temperature and the thermal gradient distributions. The finite difference method, described briefly in the following section, will be used to solve the heat equation because of its relative simplicity in the case of pure conduction problem in 2D.

Boichot R., Luo L., and Fan Y. Tree-network structure generation for heat conduction by cellular automaton. Energy Conversion and Management, 50(2):376–386, 2009.

---

*2.1. Theoretical background*

The method used here for solving the heat equation is the centered finite difference scheme with five points (Fig. 1.). The heat equation for a material in non-stationary conditions is written as follows:

$$\rho C_p \frac{\partial T(x,y,t)}{\partial t} = \lambda \Delta T(x,y,t) + p(x,y,t) \tag{1}$$

Where $\rho$, $Cp$, $\lambda$ and $p$ stand for density (kg $m^{-3}$), heat capacity (J $kg^{-1}K^{-1}$), thermal conductivity (W $m^{-1}K^{-1}$) and heat generation rate per unit volume (W $m^{-3}$) of the material respectively. They are considered as constant physical properties during the calculation.

By developing the partial derivatives of temperature in space and time as a Taylor expansion, ignoring the third-order derivatives and considering the $\Delta t$ and $\Delta x$ as small differences, the well-known expression of centered temperature for finite difference in five centered points is obtained:

$$T(x,y,t+\Delta t) = T(x,y,t) + \Delta t \left[ \begin{array}{l} a \dfrac{T(x-\Delta x,y,t) + T(x+\Delta x,y,t) + T(x,y-\Delta x,t) + T(x,y+\Delta x,t)}{(\Delta x)^2} \\ - a \dfrac{4T(x,y,t)}{(\Delta x)^2} + \dfrac{p(x,y,t)}{\rho C_p} \end{array} \right] \tag{2}$$

Boichot R., Luo L., and Fan Y. Tree-network structure generation for heat conduction by cellular automaton. Energy Conversion and Management, 50(2):376–386, 2009.

---

The forward Euler algorithm is used here for integration (also called explicit time stepping). We therefore only need the temperature field values of the previous time step or initially a given temperature distribution to calculate those of the following steps.

Eq. (2) is exact as long as the materials of the four cells surrounding the central cell have the same thermal conductivity. Generally speaking, each temperature must be weighted by global conductance between nodes. Let us consider the case of Fig. 1, which presents a central node and four surrounding ones and their equivalent thermal resistance net (elemental calculation assembly for this finite difference method).

Note that the thermal conductivity $\lambda$ of each cell around the central cell can have a different value. Balancing the heat flux at the central node in a non-stationary state, taking into account each thermal resistance between nodes, and changing the indices according to Fig. 1 for simplification gives:

$$\rho_1 C_{p1} (\Delta x)^2 (T_{1,t+\Delta t} - T_{1,t}) = [Q_{1\to 2} + Q_{1\to 3} + Q_{1\to 4} + Q_{1\to 5} + p_1(t)(\Delta x)^2]\Delta t \qquad (3)$$

$$Q_{1\to i} = K_{1\to i}(T_{i,t} - T_{1,t}) \qquad (2\leq i\leq 5) \qquad (4)$$

$$K_{1\to i} = \frac{\Delta x}{\frac{\Delta x/2}{\lambda_1} + \frac{\Delta x/2}{\lambda_i}} \qquad (2\leq i\leq 5) \qquad (5)$$

Where $K_{1\to i}$ and $Q_{1\to i}$ stand for the thermal conductance (W $m^{-1}K^{-1}$) and the heat flux transferred (W $m^{-1}$) between the central cell 1 and its neighboring cell *i* at the time *t*. Rearranging the equation (3) to replace $Q_{1\to i}$ leads to:

$$T_{1,t+\Delta t} = T_{1,t} + \Delta t \left[ \frac{p_1(t)}{\rho_1 C_{p1}} + \frac{\sum_{i=2}^{5} K_{1\to i}(T_{i,t} - T_{1,t})}{\rho_1 C_{p1}(\Delta x)^2} \right] \quad (6)$$

Eq. (6) reduces to Eq. (2) in case that the thermal resistances $\lambda_i$ between all nodes are equal. In a stationary state, this equation reduces to:

$$p_1(t)(\Delta x)^2 + \sum_{i=2}^{5} K_{1\to i}(T_i - T_1) = 0 \quad (7)$$

$$T_1 = \frac{\sum_{i=2}^{5} K_{1\to i} T_i + p_1(t)(\Delta x)^2}{\sum_{i=2}^{5} K_{1\to i}} \quad (8)$$

Lastly, the norm of the thermal gradient at each node, which is the "attractive quantity" for cellular automaton, is evaluated at the temperature equilibrium by the following equation (indices according to Fig. 1):

$$\left\| \overrightarrow{grad} T_1 \right\| = \sqrt{\left( \frac{T_3 - T_5}{2\Delta x} \right)^2 + \left( \frac{T_2 - T_4}{2\Delta x} \right)^2} \quad (9)$$

Eqs (6) and (8) are applied at each node of the calculation domain by iteration till the convergence of the temperature solution. The solution can require a large computation power since it has to be solved at each new cell configuration after cellular automaton is applied. To reduce the calculation time, a convergence criterion of $10^{-6}$ K is taken for the initial solution with the initial shape used as a reference for temperature, and this criterion is reduced to $10^{-2}$ K between each new cell configuration, as the shape between two step of the cellular automaton stay relatively unchanged. We choose a square of 400

Boichot R., Luo L., and Fan Y. Tree-network structure generation for heat conduction by cellular automaton. Energy Conversion and Management, 50(2):376–386, 2009.

---

$\times$400 cells as the calculation domain in order to limit a reasonable calculation delay. Note that higher resolution can be achieved provided with more powerful computational machines.

*2.2. Boundary conditions / cell property*

Four kinds of square cells are defined to cover the entire calculation domain in order to simulate the heating square problem. Each kind of cell used is now described:

- *Heat sink cells:* cells that have a constant temperature and a thermal conductivity equal to $k_p$ (thermal conductivity of high conductivity material). These cells must occupy a small part of the domain boundary to create the point-like heat sink;
- *Adiabatic cells*: cells that have a floating temperature and a very low conductivity ($10^{-9}$ W $m^{-1}K^{-1}$). These cells must enclose all the domain except the heat sink area;
- *High conductivity non heating cells*: cells that form the conductive tree with $k_p$ conductivity and zero heat generation rate, linked to the heat sink;
- *Low conductivity heating cells*: heat generating cells that by default cover the entire remaining domain with $k_0$ (thermal conductivity of high conductivity material).

The only strict constraint is to ensure that adiabatic and heat sink cells enclose the complete calculation domain. Only the conductive cells are moved during the cellular automaton procedure. Concretely, the calculation domain is drawn with a graphical tool (in a Portable Pixmap file), each pixel color corresponding to a cell type. The

calculation code is then able to interpret this image as a calculation domain for the start-up.

*2.3. Choice of an initial shape*

Technically, all possible domain geometries with different initial shapes of high conductivity material can be simulated with this code. To illustrate the cellular automaton procedure in a directive and descriptive manner, we find it interesting, as said in introduction section, to use as initial shape the dichotomic tree with perpendicular branches optimized analytically by Constructal theory [3]. Table 1 gives the five shapes that will be tested as initial shape to evaluate the performance of cellular automaton (indices according to [3]). Because of the paper length limitation, we will not repeat here the procedure of the formation of constructal dichotomic tree-network. Complete explanation of the optimization and assemble procedure can be found in [3].

Shapes 1 to 4 in Table 1 are classical dichotomic trees with 4 levels of branching, whereas Shape 5 has the same composition in terms of $\hat{k}$ and $\phi_0$ as that of the shape 4 but organized randomly in stead of the dichotomic tree type. The parameter $\hat{k}$ tested in our cases covers a range from 50 to 200. Shapes 1 and 2 will give an estimation of the effect of the parameter $\phi_0$ whereas Shapes 2, 3 and 4 will illustrate the effect of $\hat{k}$ ratio. The comparison of Shapes 4 and 5 will highlight the influence of initial shape on final configuration obtained.

*2.4. Operation of the cellular automaton*

Boichot R., Luo L., and Fan Y. Tree-network structure generation for heat conduction by cellular automaton. Energy Conversion and Management, 50(2):376–386, 2009.

---

As highlighted above, the principle proposed attempts to evolve the structure of the high conductivity link only according to the local criterion: the thermal gradients at its frontier. This empirically imitates the growth of a conductive tree that is attracted by thermal gradients. It is conjectured that adding high conductivity material where thermal gradients are high against the frontier will support the growth of branches toward high temperature region and will locally facilitate the heat conduction. As a result, a decrease of the maximal temperature is expected. Similarly, if thermal gradients are locally low against the frontier, the high conductivity material could be dismantled without strong differences in heat flux distribution. By displacing the same quantity of high conductivity material from regions of low thermal gradients to regions of high thermal gradients, the total number of conductive cells keeps unchanged during calculation as shown in Fig. 2. Improving the effectiveness of high conductivity material in this manner ensures that at the convergence, the heat flux density becomes equally distributed across the frontier.

Practically speaking, the complete calculation code is written as explained in Fig. 3. The first step of the cellular automaton consists in obtaining the temperature and thermal gradient distributions of the initial shapes with a convergence criterion of $10^{-6}$ K. The second step consists in moving cells with high conductivity material each time till thermal equilibrium is reached (convergence criterion: $10^{-2}$ K). After many trails, we found that the solver gives a convergent configuration, nearly not influenced by initial shape, after 300 moving steps and a moving rate of 50%* of the cells with high

---

We also found that the shape converges easily on condition that the moving rate is linearly reduced from 50% at the beginning to 0% at the 300$^{th}$ step. This "optimal condition" seems to be almost independent on

conductivity material at the beginning. The moving rate is defined as the ratio of the number of conductive cells that are allowed to move and the total number of conductive cells at each step.

This calculation procedure has mainly two particularities. The first is that the number of conductive cells moving at each step can be relatively large (up to several tenth percents of the number of conductive cells), which may considerably reduce the calculation time. The second is that the convergence criterion for temperature can be relatively coarse, because even if the moving rate is high, the frontier can only move cells layer by layer, ensuring only little differences in the tree shape between each cellular automaton step.

## 3. Results and discussion

Maximal temperatures in the square surface case are always situated at the two corners opposite to the heat sink. The ratio of the maximal temperature to the initial maximal temperature of the area at each step is calculated. Fig. 4 gives a plot of the evolution of this ratio during the convergence for each shape tested. Figs 5a, 6a, 7a, 8a and 9a give the evolution of high conductivity link configuration with cellular automaton for Shapes 1, 2, 3, 4 and 5 respectively, in the way of natural reading for the $1^{st}$, the $16^{th}$, the $32^{th}$ , the $75^{th}$ , the $150^{th}$ and the $300^{th}$ step of calculation. High conductivity material ($k_p$) is represented by black cells and heat producing material ($k_0$) by white ones. Figs 5b, 6b, 7b, 8b and 9b illustrate the initial and final aspects of temperature and thermal gradients

the number of cells in the calculation domain and the physical properties of the high conductivity material. Further studies are needed to give a definite explanation on this point.

distributions of the calculation domain. In these figures, the greyscale is linear and reduced according to the minimal and maximal values calculated for each initial shape tested.

It can be observed that for certain initial shapes with proper $\hat{k}$ and $\phi_0$, the cellular automaton algorithm leads to completely different final configurations, which turn out to be natural tree-network structure and similar to those of Errera and Bejan [11] in global view. The trees generated contain at most three levels of bifurcation, without any sort of perpendicular dichotomic structures. Note that the temperature distributions and conductive trees obtained are not completely symmetrical. This is mainly due to the iteration procedure by scanning cells, which starts from the upper left border and proceeds towards the lower right border. This leads to a slight initial dissymmetry in temperature distribution that is amplified by an asymmetrically cells moving. Finally the shapes obtained are symmetrical in global but diverse in detail.

*3.1. Decrease in maximal temperature of the domain*

From the Fig. 4, it can be observed that the ratio of the maximal temperature during the shape morphing passes through a maximum value before it decreases. The tendency is obvious, in particular for Shape 1 whose initial maximal temperature is finally reached only at the end of the morphing process. This is mainly due to the high moving rate used: the initial smallest tree branches are rapidly and completely destroyed during a few starting steps (attacked by their side, cells layer by cells layer). However, the reconstruction of the tree-network in small scale needs numerous steps (constructed by their tips, cell layer by cell layer); this leads to certain “blank” areas without high

conductivity drains during several tenth of moving steps. As a result, the maximal temperature would show an increasing tendency during the first part of calculation steps before it decreases, regarding the coding of the algorithm.

The ratio between final and initial maximum temperature ($T_{max}$ / $T_{max\ initial}$, reduced temperature) is 99.8% for Shape 1, 71.6% for Shape 2, 72.0% for Shape 3, 64.9% for Shape 4 and 27.5% for Shape 5 respectively. Note that this primary divergence is strongly linked to the initial shape. We can consider that for Shape 1 there is no significant improvement during the chosen 300 calculation steps. A smaller final $T_{max}$ / $T_{max\ initial}$ is expected if continued more calculation steps are provided since it still shows a decreasing tendency. On contrary, as to the case of Shape 5, the random initial shape of isolated conductive isles is so bad for heat conduction that each moving step of cellular automaton leads to a better configuration. So, the reduced temperature decreases almost continuously during the morphing process. The influence of the initial shape will be discussed in detail in the later section.

It is necessary to explain in what sense the thermal gradient equalization can also approach the minimization of the maximal temperature. In this kind of problem, the maximal temperature minimization is achieved only when the temperatures against the adiabatic external boundaries of the domain are equalized. This is not a priori a waited result or a goal of the cellular automaton. But we also observed that the thermal gradients equalization at the frontier between the two materials and the temperature equalization at the adiabatic borders coincide under high $\hat{k}$ ratio conditions (thermal resistance of the conductive link negligible compared to the heating part of strips).

Boichot R., Luo L., and Fan Y. Tree-network structure generation for heat conduction by cellular automaton. Energy Conversion and Management, 50(2):376–386, 2009.

---

*3.2 Effect of the ratio of thermal conductivity* $\hat{k}$

The effect of the ratio of thermal conductivity between high and low conductivity materials ($\hat{k}=k_p/k_0$) is presented by simulation results. By comparing the evolutionary pictures of Shape 2 and Shape 4 which have approximately the same initial quantity of high conductivity material, we observe that the lower the $\hat{k}$ is, the faster the convergence of the configuration can be obtained. We think that this convergence difference is mainly due to a meshing limitation: the finest branches (a dominant role for heat transfer) that can be constructed during morphing of Shape 2 have a dimension close to a cell size. It can be seen on figure 6a that the high conductivity material tends to be dispersed in the calculation domain, the formation of fin branches is difficult. In fact for $\hat{k}$ = 200, the 400×400 cells domain seems to be too coarse to permit a smooth convergence of the final configuration. For $\hat{k}$ = 50, on the other hand, the primary branches are slenderer and numerous, and small scale branches that mobilize a little quantity of high conductivity material seem not play a crucial role for heat conduction. As the primary branches are largely thicker than a cell size, their formation is not at all limited by discretisation of the domain.

This trend is particularly obvious in fig. 10, where the cellular automaton is applied in a similar manner but by starting from one and only unspecified dichotomic tree (not optimized for a $\hat{k}$ or $\phi_0$ ratio) and varying strongly the $\hat{k}$ ratio. The shapes obtained at convergence highlight the latter trends exposed. Fig. 10 is obviously given as an

illustration only, since there is no possible full and fair comparison between cellular automaton and Constructal dichotomic trees in such a large range of $\hat{k}$.

In a sense, if the discretisation rate can be high, then there is no upper limit of $\hat{k}$. And practically, there is no lower limit for $\hat{k}$ too, but the lower this value is, the less efficient is the final configuration in term of maximal temperature decreasing. We found that around $\hat{k} = 5$, it is possible to find simple configurations that are more efficient than the result of cellular automaton, since generated branches tend to not cover the entire calculation domain, as can be seen on Fig. 10.

By comparing Figs. 6 and 8, or considering Fig. 10, it can be observed that the final configurations forms thicker primary branches and more small secondary branches if the $\hat{k}$ ratio is high, better covering the space allowed for the branches. This is an interesting characteristic of this algorithm: the more the temperature can be reduced in the domain (high $\hat{k}$), the more efficient becomes the tree-network generated to occupy the entire space.

*3.3 Effect of the fraction of high conductivity material* $\phi_0$

While the $\hat{k}$ ratio signifies the quality of the high conductivity material, the fraction $\phi_0$ indicates its quantity over the area studied. By comparing Shape 1 and 2 ($\hat{k} = 200$, $\hat{k}\varphi_0 =$ 4 and 16 respectively), the $\phi_0$ parameter seems to play a dominant role in shape

morphing. The higher the $\phi_0$ is, the thicker become the branches for a same $\hat{k}$ ratio. In case of a small $\phi_0$ value, the level of branching increases and the smallest branches tend to elongate themselves to reach high temperature regions, progressing cells by cells during the cellular automaton procedure. This leads to a final shape that strongly depends on discretisation rate. We think this is the main cause of the inefficiency of final tree generated with shape 1.

On the other hand, for Shapes 2 and 4, where the initial quantity of high conductivity material reaches several tenth percents on the whole domain, the finest branches are not immediately dismantled at the beginning of the morphing process and contribute immediately to the formation of new branches (see Fig. 8a where the phenomenon is clearly visible). Finally, a configuration with thicker primary branches and a low branching level is formed at convergence.

By comparing Figs. 5-8, it can be observed that for certain values of $\hat{k}$ and $\phi_0$, the progressive increase of internal branching level (higher complexity) seems not necessary to obtain a “better” thermal performance. The thick primary branches are directly connected with small branches without many intermittent scales, as shown on the final configuration of Shape 4. The internal complexity found with this automaton is clearly not infinite. In the case of $\hat{k}$=50 (Fig. 8a), only two levels of branching are found at convergence, with a better thermal efficiency than that of the initial shape with four levels of branching. Fig. 10 gives a comparison of the final configurations starting with the same constructal perpendicular initial shape but with different $\hat{k}$ between 200

---

and 2. It is clear that the smaller the $\hat{k}$ is, the less complex the final configuration becomes (lower branching level). *In a sense, the branching level of the tree-network, or the level of complexity, is also a parameter for optimization.* The optimal branching level, as well as the optimal geometric structure depends on global and local constraints and in this case the $\hat{k}$ and $\phi_0$, etc. Similar comments on the level of complexity can also be found in a recent review of Kuddusi and Egrican [13]

*3.4 Effect of the initial shape*

By comparing Shapes 4 and 5 having the same physical properties of high conductivity material, the influence of the initial shape is highlighted. Shape 4 is already optimized analytically by Constructal theory and Shape 5 is an unspecified accumulation of non-linked high conductivity material blocks. It can be observed that by applying the cellular automaton algorithm, the two shapes evolve toward nearly the same final configuration, but not exactly. The final maximal temperature of shape 5 is 19% higher compared to that of the Shape 4. This might be due to the fact that the iteration process (in step number or moving rate) is too short to obtain one and only configuration from many different initial shapes.

But even with this deficiency, the final maximal temperature of shape 5 is 20% lower than the initial maximal temperature of shape 4. Note that the initial shape 4 is already optimized analytically by constructal theory. That is to say, the cellular automaton approach is at least as efficient as the analytical Constructal theory in this case.

Boichot R., Luo L., and Fan Y. Tree-network structure generation for heat conduction by cellular automaton. Energy Conversion and Management, 50(2):376–386, 2009.

## 4. General comments on cellular automaton algorithm

Compared to the analytical developments of Constructal theory limited to simple symmetrical shapes, the main advantage of the cellular automaton keeps its relative absence of geometric constraints. The optimal solution is built directly from the overall area to cool or drain, with the only constraint of certain quantity (quality) of high conductivity material to shape. In this paper, only a square area example is presented, but technically any geometry could be very easily treated with this approach with the help of the common graphical tools, simply by adding sink and sources, adiabatic boundaries into the domain, and adjusting the physical properties of high conductivity material. A direct extension for a cylindrical geometry was given by Boichot and Luo [14]. We are studying other applications such as unspecified domains possibly containing multi-sources or sinks of heat. Moreover, when dealing with actual electronic engineering cases, more realistic configurations could be generated by taking into account some contact resistances between the poorly and highly conductive materials. In a word, this approach is convenient, adaptive to unspecified geometries and easy to implement in dealing with the heat conduction problem.

A main limitation is that the obtained complex structure by this method is difficult to realize at current stage in view of the direct engineering application. As a result, the breakthroughs in manufacture technologies and improvements in fabrication accuracy are in need. And also, because of the discrete formulation, at most three levels of branching tree-network are observed in our cases. As we have mentioned above, the

branching level, or the level of complexity, is a parameter for optimization. To make a comprehensive investigation of this point in detail, a finer mesh is in need.

## 5. Conclusion and perspectives

To conclude, what we do here is only to propose a simple algorithm "the morphing by gradients attraction" to attack the case of cooling a heat generating surface by conduction. With very simple assumptions and basic rules, the algorithm which equalizes the thermal gradients at the frontier between high and low conductivity materials leads to the emergence of tree-network configuration, without any constraint other than the shape of the external boundary of the domain. The approach may not continuously decrease the maximal temperature in a strict mathematical point of view, but the comparison with the results of analytical Constructal theory indicates that in all tested cases, the configurations proposed by the cellular automaton are at least as performing as those proposed by Constructal theory. The cellular automaton algorithm is convenient, adaptive to unspecified geometries and easy to implement for the optimization of heat conduction in a surface.

For perspectives, the first extension is to investigate heat conduction optimization in unspecified domains possibly containing multi-sources or sinks, with higher cellular resolution and more calculation steps to obtain more precise results. Secondly, in view of the general "area-to-point" problem, what flows in the domain is of the second importance. In principle, the cellular automaton approach may also be extended to various physical problems, for example heat convection, formation of river basin, or

Boichot R., Luo L., and Fan Y. Tree-network structure generation for heat conduction by cellular automaton. Energy Conversion and Management, 50(2):376–386, 2009.

---

even the arrangement of streets for transportation, with the modifications of the code with proper mathematical formulations. And finally, could this algorithm be extended for the simulation of nature processes? Some thoughts of cellular automaton application in biology can be found in [15, 16]. This certainly needs more effective interactions and cooperation between the various sections of the research field.

## Acknowledgments

This work is supported by the French ANR (Agence National de la Recherche) within the “programme non thématique 2005, Projet n°NT05-3_41570). The authors want to thank Dr. Daniel Tondeur (CNRS-Nancy) for fruitful discussions and criticisms.

Boichot R., Luo L., and Fan Y. Tree-network structure generation for heat conduction by cellular automaton. Energy Conversion and Management, 50(2):376–386, 2009.

## Nomenclature

| | | |
|---|---|---|
| $a$ | Thermal diffusivity | $m^2 s^{-1}$ |
| $C_p$ | Heat capacity | $J kg^{-1}K^{-1}$ |
| $i$ | Indices | - |
| $K$ | Thermal conductance between cells | $W m^{-1}K^{-1}$ |
| $k_p$ | Thermal conductivity of highly conductive material | $W m^{-1}K^{-1}$ |
| $k_0$ | Thermal conductivity of heat generating material | $W m^{-1}K^{-1}$ |
| $\hat{k}$ | Ratio between $k_p$ and $k_0$ | - |
| $Q$ | Heat flux between cells | $W m^{-1}$ |
| $T$ | Temperature | K |
| $T_i$ | Temperature at node i | K |
| $p$ | Heat generation rate per unit volume | $W m^{-3}$ |
| $t$ | time | s |
| x, y | Cartesian coordinates | - |

*Greek symbols*

| | | |
|---|---|---|
| $\lambda$ | Thermal conductivity | $W m^{-1}K^{-1}$ |
| $\lambda_i$ | Thermal conductivity at node i | $W m^{-1}K^{-1}$ |
| $\phi_0$ | Volume fraction of high conductivity material at elemental scale | - |
| $\rho$ | Density | $kg m^{-3}$ |

Boichot R., Luo L., and Fan Y. Tree-network structure generation for heat conduction by cellular automaton. Energy Conversion and Management, 50(2):376–386, 2009.

---

## References

[1] Bejan A, Lorente S. Constructal theory of generation of configuration in nature and engineering. J Appl Phys 2006;100:041301.

[2] Bejan A. Shape and Structure, from engineering to nature. Cambridge: Cambridge University Press; 2000, ISBN 0 521 79049 2.

[3] Bejan A. Conctructal theory network of conducting paths for cooling a heat generating volume. Int J Heat Mass Transfer 1997;40:799-816.

[4] Wu W, Chen L, Sun F. On the “area to point” flow problem based on constructal theory. Energy Convers Manage 2006;48:101-5.

[5] Rocha LOA, Lorente S, Bejan A. Constructal design for cooling a disc-shaped area by conduction. Int J Heat Mass Transfer 2002;45:1643-52.

[6] Ghodoossi L. Conceptual study on constructal theory. Energy Convers Manage 2004;45:1379-95.

[7] Ghodoossi L, Egrican N. Conductive cooling of triangular shaped electronics using constructal theory. Energy Convers Manage 2004;45:811-28.

[8] Zhou S, Chen L, Sun F. Optimization of constructal volume to point conduction with variable cross section conducting path. Energy Convers Manage 2006;48:106-11.

[9] Lorenzini G, Rocha LOA. Constructal design of Y-shaped assembly of fins. Int J Heat Mass Transfer 2006;49:4552-7.

---

[10] Ledezma GA, Bejan A, Errera MR. Constructal tree networks for Heat transfer. J Appl Phys 1997;82:89-100.

[11] Errera MR, Bejan A. Deterministic tree network for river drainage basins. Fractals 1998;6:245-61.

[12] Wolfram S. A new kind of science. Wolfram Media Inc;2002.ISBN 1-57955-008-8.

[13] Kuddusi L, Egrican N. A critical review of constructal theory. Energy Convers Manage 2007; Article In Press, available online.

[14] Boichot R, Luo L. Heat transfer intensification using a cellular automaton. Proceeding of 5th Annual Heat Transfer, Fluid Dynamics and Thermodynamics Conference (HEFAT), South Africa, 1-4 July 2007.

[15] Plantefol. L. Biologie Cellulaire et Végétale. Librairie Classique Eugène Belin ;1959.

[16] Peak D, West JD, Messinger SM, Mott KA. Evidence for complex, collective dynamics and emergent, distributed computation in plants. Proceedings of the National Institute of Science of the USA 2004;101:918-22.

Boichot R., Luo L., and Fan Y. Tree-network structure generation for heat conduction by cellular automaton. Energy Conversion and Management, 50(2):376–386, 2009.

## Figure captions

Fig. 1. Finite difference discretisation of space and the equivalent thermal resistance net used.

Fig. 2. Three steps example to illustrate the cellular automaton algorithm.

Fig. 3. Detailed calculation algorithm for cellular automaton.

Fig. 4. Reduced maximal temperatures during optimization for the different shapes studied.

Fig. 5a. Shape 1 evolution from the first to the 300th step.

Fig. 5b. Shape 1 aspect of initial and final thermal temperature and gradient fields.

Fig. 6a. Shape 2 evolution from the first to the 300th step.

Fig. 6b. Shape 2 aspect of initial and final thermal temperature and gradient fields.

Fig. 7a. Shape 3 evolution from the first to the 300th step.

Fig. 7b. Shape 3 aspect of initial and final thermal temperature and gradient fields.

Fig. 8a. Shape 4 evolution from the first to the 300th step.

Fig. 8b. Shape 4 aspect of initial and final thermal temperature and gradient fields.

Fig. 9a. Shape 5 evolution from the first to the 300th step.

Fig. 9b. Shape 5 aspect of initial and final thermal temperature and gradient fields.

Fig. 10. Results of optimization starting from an unspecified perpendicular dichotomic tree: evolution of shape according to $\hat{k}$

Boichot R., Luo L., and Fan Y. Tree-network structure generation for heat conduction by cellular automaton. Energy Conversion and Management, 50(2):376–386, 2009.

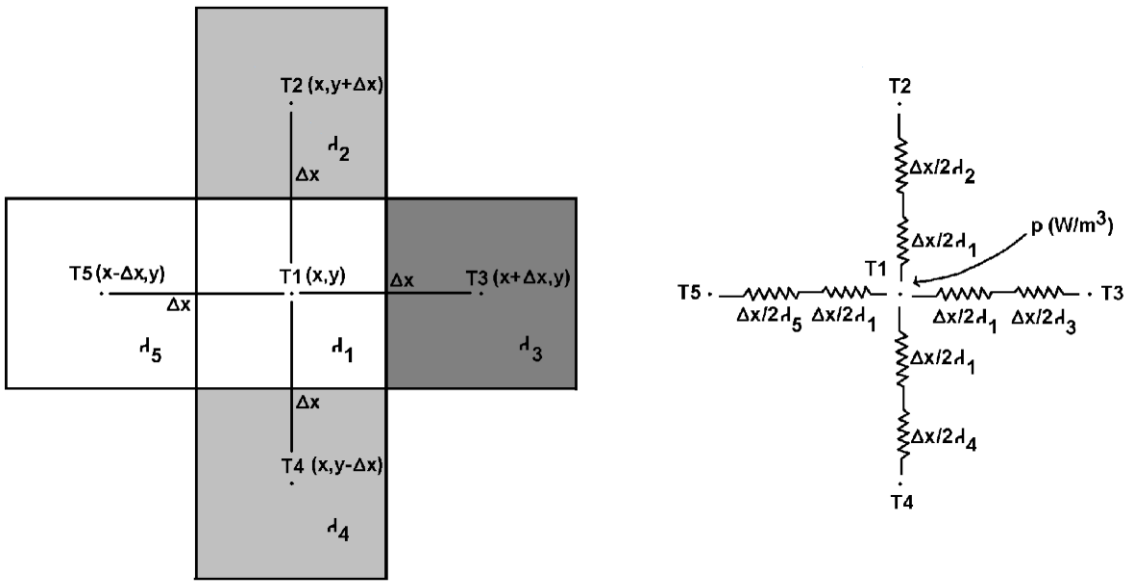


Fig. 1. Finite difference discretisation of space and the equivalent thermal resistance net used.

Boichot R., Luo L., and Fan Y. Tree-network structure generation for heat conduction by cellular automaton. Energy Conversion and Management, 50(2):376–386, 2009.

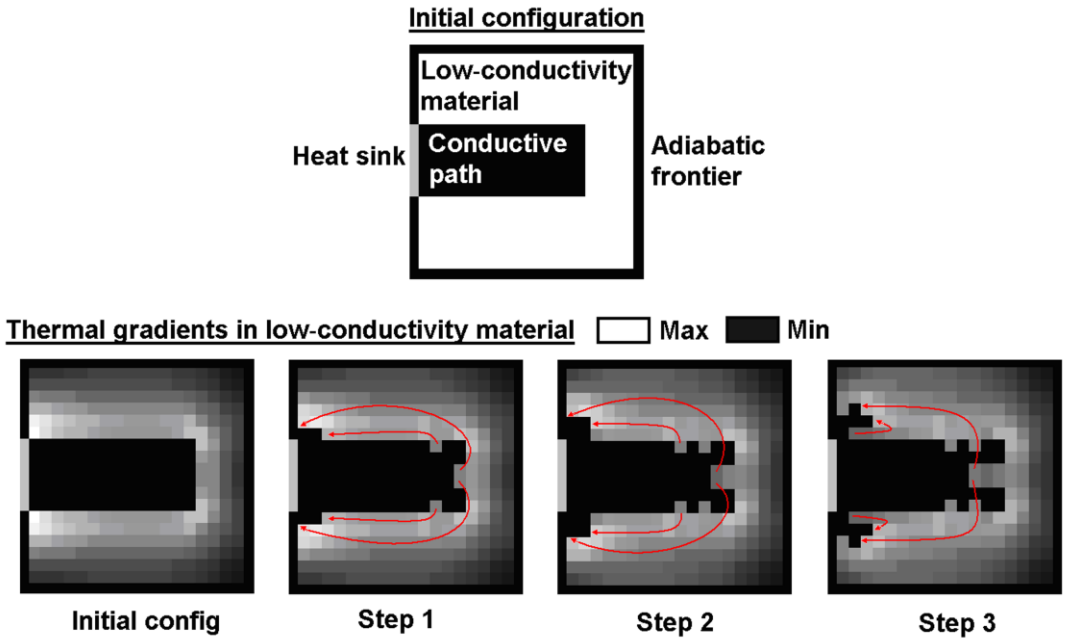


Fig. 2. Three steps example to illustrate the cellular automaton algorithm.

Boichot R., Luo L., and Fan Y. Tree-network structure generation for heat conduction by cellular automaton. Energy Conversion and Management, 50(2):376–386, 2009.

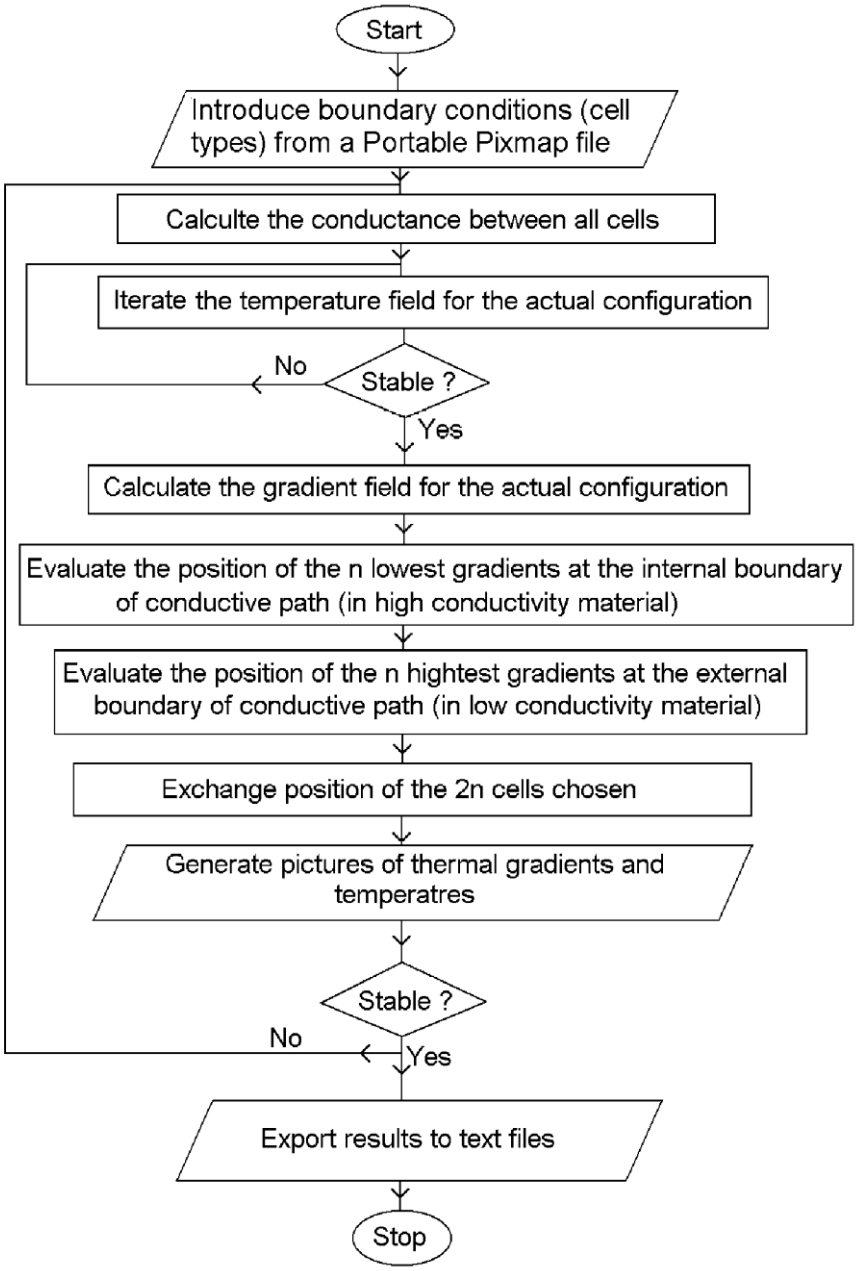


Fig. 3. Detailed calculation algorithm for cellular automaton.

Boichot R., Luo L., and Fan Y. Tree-network structure generation for heat conduction by cellular automaton. Energy Conversion and Management, 50(2):376–386, 2009.

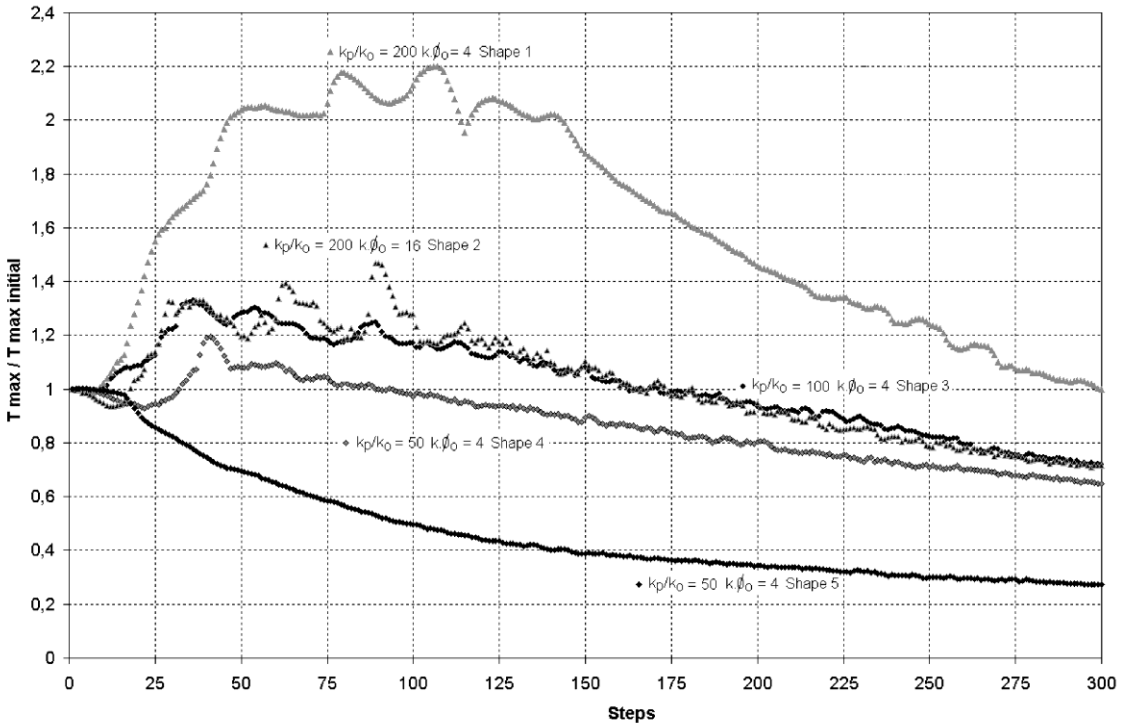


Fig. 4. Reduced maximal temperatures during optimization for the different shapes studied.

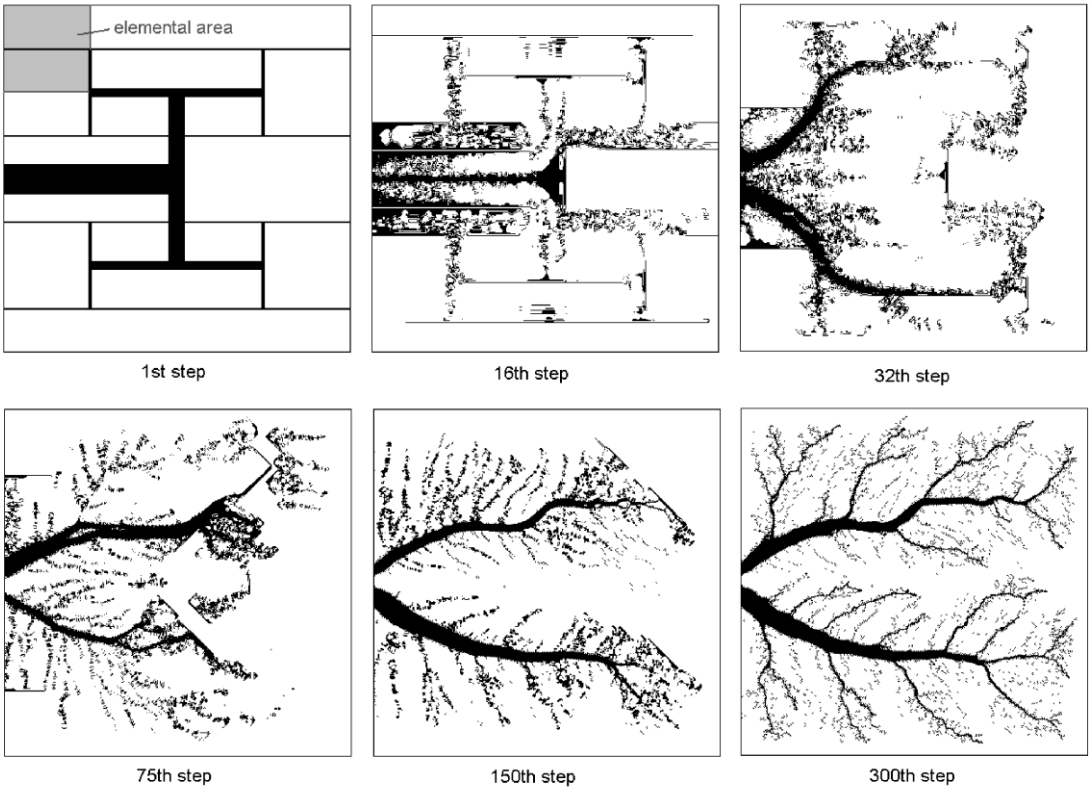


Fig. 5a. Shape 1 evolution from the first to the 300th step.

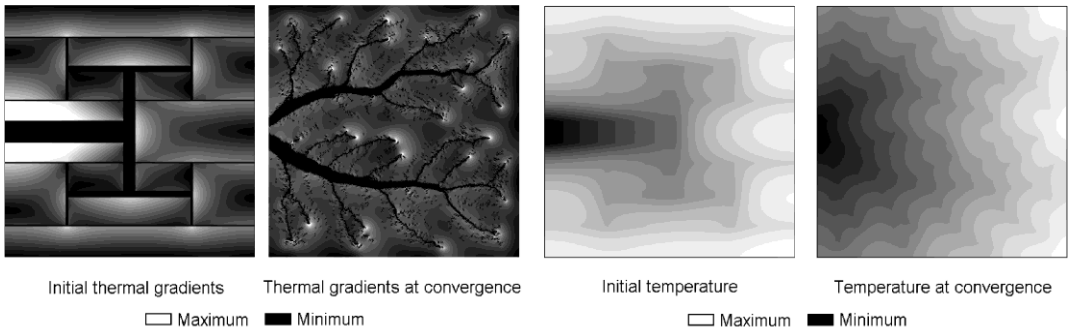


Fig. 5b. Shape 1 aspect of initial and final thermal temperature and gradient fields.

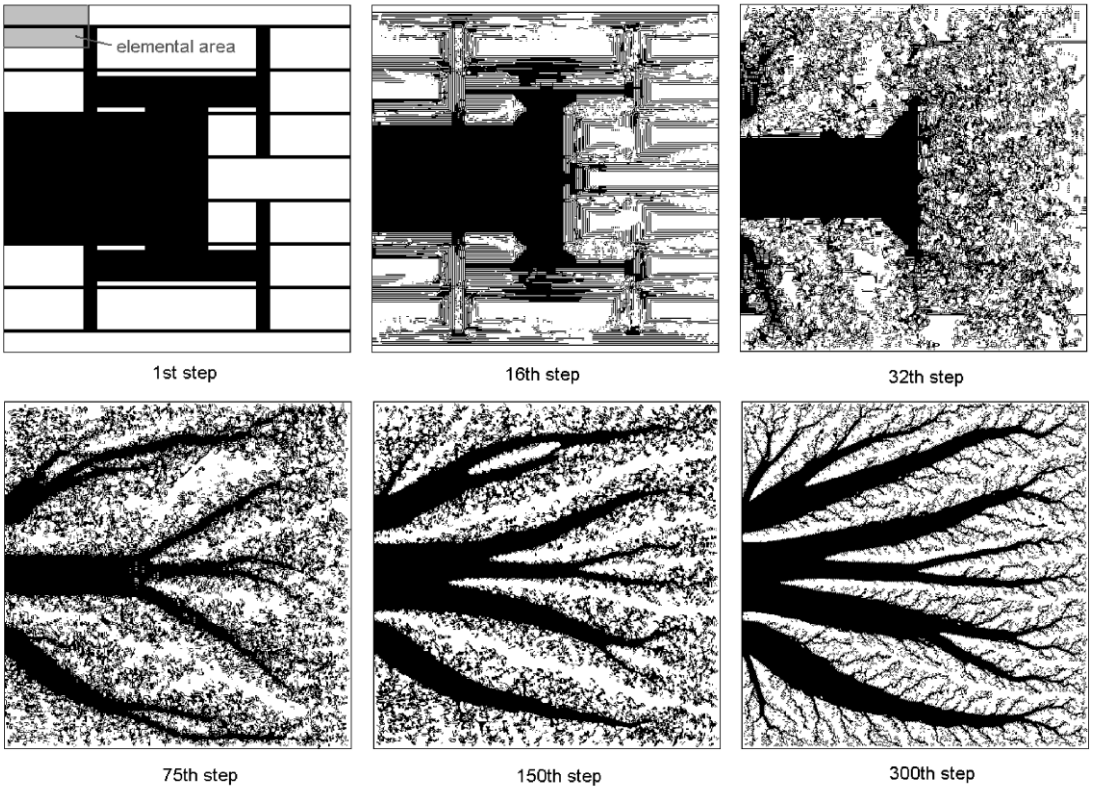


Fig. 6a. Shape 2 evolution from the first to the 300th step.

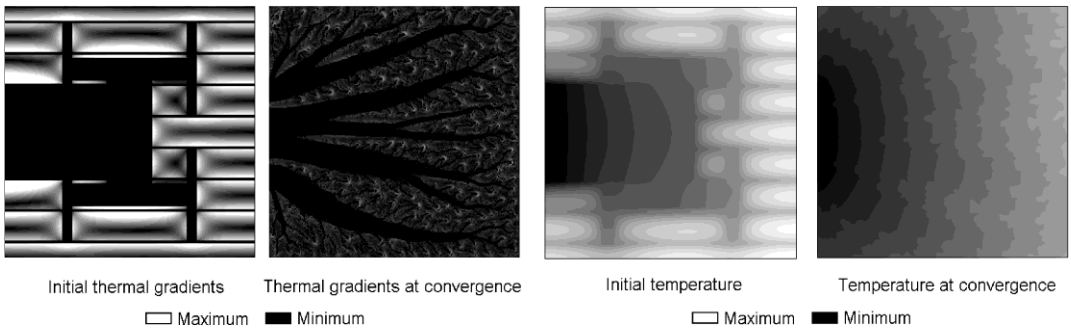


Fig. 6b. Shape 2 aspect of initial and final thermal temperature and gradient fields.

Boichot R., Luo L., and Fan Y. Tree-network structure generation for heat conduction by cellular automaton. Energy Conversion and Management, 50(2):376–386, 2009.

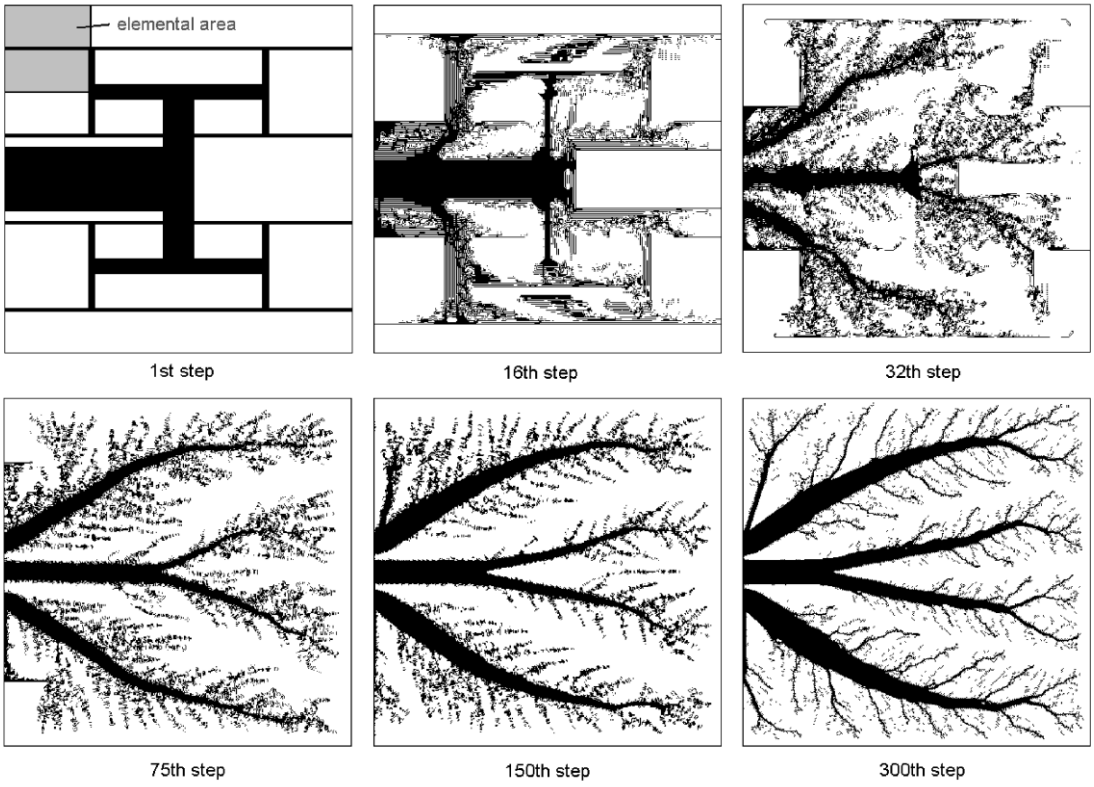


Fig. 7a. Shape 3 evolution from the first to the 300th step.

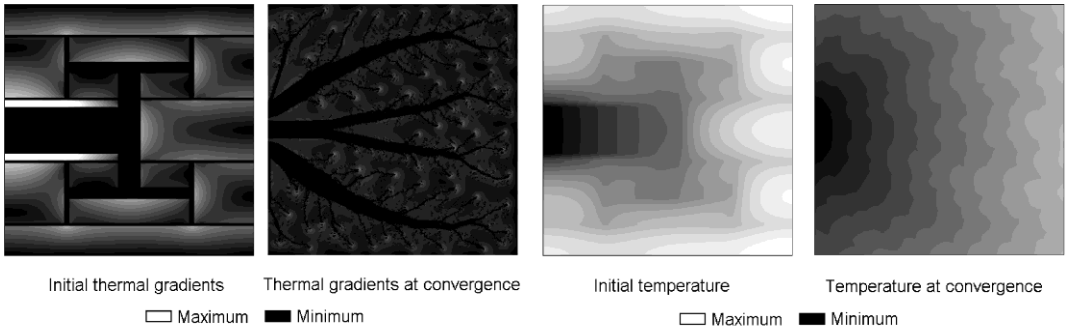


Fig. 7b. Shape 3 aspect of initial and final thermal temperature and gradient fields.

Boichot R., Luo L., and Fan Y. Tree-network structure generation for heat conduction by cellular automaton. Energy Conversion and Management, 50(2):376–386, 2009.

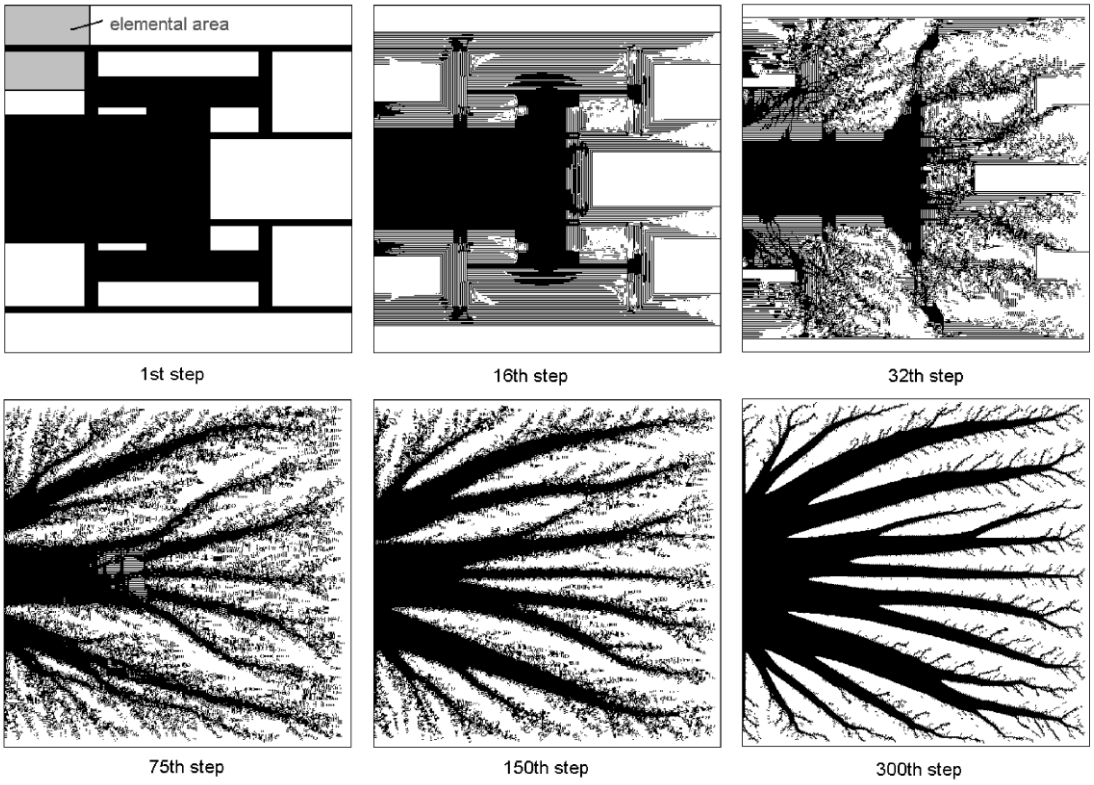


Fig. 8a. Shape 4 evolution from the first to the 300th step.

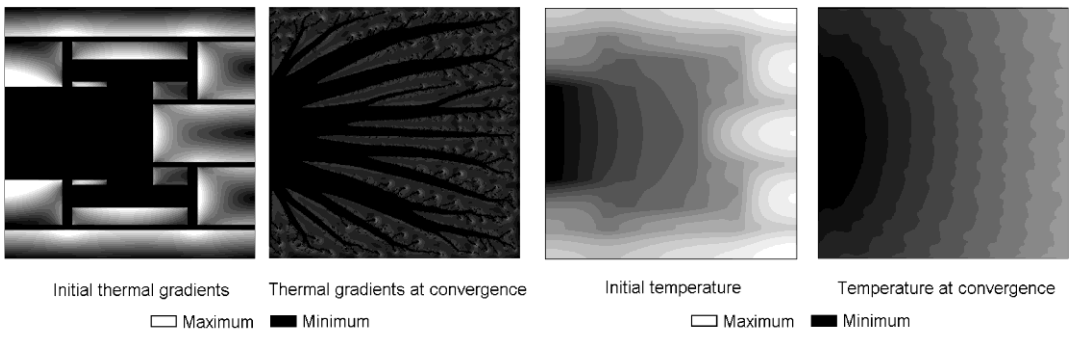


Fig. 8b. Shape 4 aspect of initial and final thermal temperature and gradient fields.

Boichot R., Luo L., and Fan Y. Tree-network structure generation for heat conduction by cellular automaton. Energy Conversion and Management, 50(2):376–386, 2009.

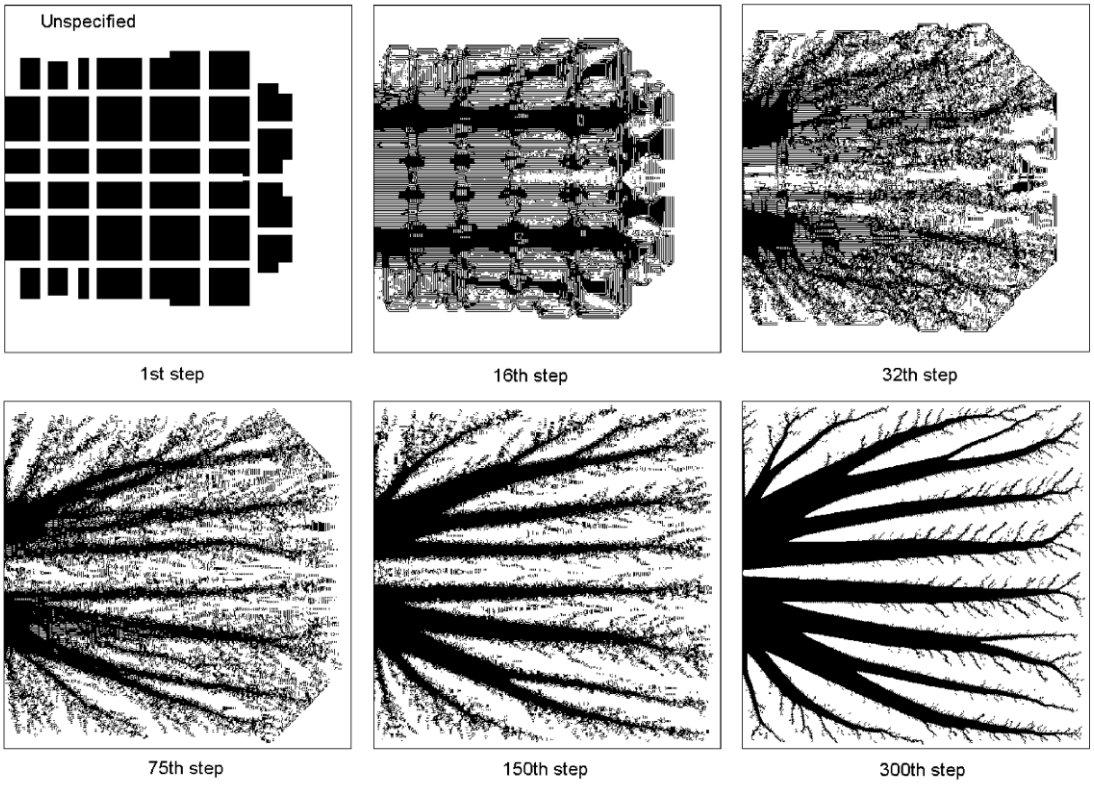


Fig. 9a. Shape 5 evolution from the first to the 300th step.

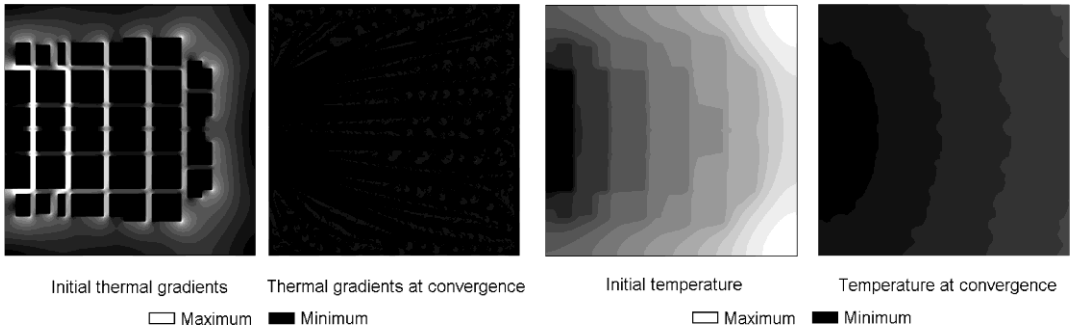


Fig. 9b. Shape 5 aspect of initial and final thermal temperature and gradient fields.

Boichot R., Luo L., and Fan Y. Tree-network structure generation for heat conduction by cellular automaton. Energy Conversion and Management, 50(2):376–386, 2009.

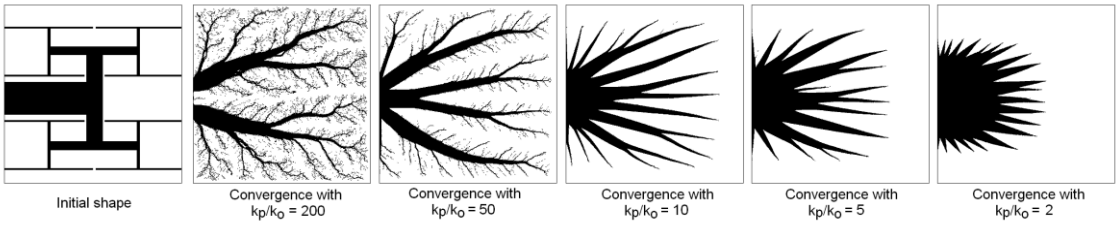


Fig. 10. Results of optimization starting from an unspecified perpendicular dichotomic tree: evolution of shape according to a large range of $\hat{k}$.

Boichot R., Luo L., and Fan Y. Tree-network structure generation for heat conduction by cellular automaton. Energy Conversion and Management, 50(2):376–386, 2009.

Table 1. Initial shapes tested by cellular automaton. Image to the right side of the figure gives the signification of indices used for the elemental area considered (according to [3])

| | Shape 1 | Shape 2 | Shape 3 | Shape 4 | Shape 5 |
|---|---|---|---|---|---|
| $k_p/k_o$ | 200 | 200 | 100 | 50 | 50 |
| $\phi_o$ | 0.02 | 0.08 | 0.04 | 0.08 | 0.08 |
| $\hat{k}\phi_o$ | 4 | 16 | 4 | 4 | 4 |
| Shape type | Constr. | Constr. | Constr. | Constr. | Unspec. |
| $H_o$ (cells) | 100 | 50 | 100 | 100 | / |
| $D_o$ (cells) | 2 | 4 | 4 | 8 | / |
| $L_o$ (cells) | 100 | 100 | 100 | 100 | / |
| Size (cells) | 400x400 | 400x400 | 400x400 | 400x400 | 400x400 |
| Heat sink size (cells) | 37 | 148 | 74 | 148 | 148 |

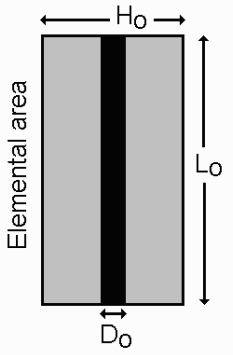


$\phi_0$: Volume fraction of high conductivity material at elemental scale.